

## Energy Distribution Function of Quasiparticles in Mesoscopic Wires

H. Pothier, S. Guéron, Norman O. Birge,\* D. Esteve, and M. H. Devoret

*Service de Physique de l'Etat Condensé, Commissariat à l'Energie Atomique, Saclay, F-91191 Gif-sur-Yvette, France*

(Received 25 April 1997)

We have measured with a tunnel probe the energy distribution function of Landau quasiparticles in metallic diffusive wires connected to two reservoir electrodes, with an applied bias voltage. The distribution function in the middle of a 1.5- $\mu\text{m}$ -long wire resembles the half sum of the Fermi distributions of the reservoirs. The distribution functions in 5- $\mu\text{m}$ -long wires are more rounded, due to interactions between quasiparticles during the longer diffusion time across the wire. From the scaling of the data with the bias voltage, we find that the scattering rate between two quasiparticles varies as  $\varepsilon^{-2}$ , where  $\varepsilon$  is the energy transferred. [S0031-9007(97)04367-6]

PACS numbers: 73.23.-b, 71.10.Ay, 72.10.-d

The present understanding of metals is based on Landau's theory of Fermi liquids. In this model, the elementary excitations of the fluid of interacting electrons are nearly independent fermionic quasiparticles [1]. In disordered metals, residual interactions between quasiparticles lead in mesoscopic samples to measurable corrections to the density of states, and limit the phase coherence of quasiparticles [2]. These effects have been widely investigated experimentally and theoretically in the last 20 years [3]. However, the most elementary manifestation of interactions, namely, the transfer of energy between quasiparticles, has been observed only at energies of order 1 eV by time-resolved spectroscopy of a metallic film following a laser pulse [4], and in the meV range through the establishment of an electron temperature in the so-called hot-electron regime [5]. Indications as to the speed at which this thermalization proceeds were obtained in recent shot noise experiments [6].

In this Letter, we report a direct measurement of the energy transfer rates between quasiparticles in diffusive metallic wires. We have measured the energy distribution function of quasiparticles in wires in a stationary out-of-equilibrium situation, at low enough temperature so that quasiparticle-quasiparticle interaction is the dominant inelastic process. The deviations of the energy distribution function from the Fermi distribution give access to the energy transfer rates. We force the wire out of equilibrium by placing it between two reservoir electrodes [7] biased at different potentials, 0 and  $U$ , as shown in Fig. 1. The local distribution function is probed with a superconducting electrode connected to the wire by a tunnel junction. The experiment exploits the property of the distribution function to have different shapes depending on the amount of inelastic collisions a quasiparticle experiences during its diffusion time through the wire.

The steady-state distribution function  $f(x, E)$  in a metallic wire of length  $L$ , which depends on the position  $X = xL$  measured from the right electrode, and on the energy  $E$ , results from the combined action of the elastic diffusion and of interactions. It obeys the Boltzmann

equation [8,9]

$$\frac{1}{\tau_D} \frac{\partial^2 f(x, E)}{\partial x^2} + I_{\text{coll}}(x, E, \{f\}) = 0. \quad (1)$$

Here  $\tau_D = L^2/D$  is the diffusion time through the wire, and  $I_{\text{coll}}(x, E, \{f\})$  is the collision integral due to the inelastic scattering processes. In the absence of electron-phonon scattering,  $I_{\text{coll}}(x, E, \{f\})$  is due to interactions between quasiparticles only. The boundary conditions are imposed by the reservoir electrodes:  $f(0, E) = [1 + \exp(\frac{E}{k_B T})]^{-1}$  and  $f(1, E) = [1 + \exp(\frac{E+eU}{k_B T})]^{-1}$ . If no scattering between quasiparticles occurs during the diffusion time, the distribution function is the solution  $f_0(x, E)$  of Eq. (1) with no collision integral [8]:

$$f_0(x, E) = (1 - x)f(0, E) + xf(1, E). \quad (2)$$

The function  $f_0(x, E)$  has a well-defined intermediate step for  $|eU| \gg k_B T$ , as shown in Fig. 1 as solid lines.

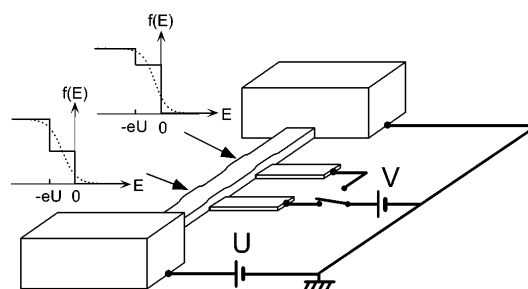


FIG. 1. Experimental layout: a metallic wire of length  $L$  is connected at its ends to reservoir electrodes, biased at potentials 0 and  $U$ . In the absence of interaction, the distribution function at a distance  $X = xL$  from the grounded electrode has an intermediate step  $f(E) = 1 - x$  for energies between  $-eU$  and 0 (solid curves) (we assume  $U > 0$ ). When interactions are strong enough to thermalize electrons, the distribution function is a Fermi function, with a space-dependent temperature and electrochemical potential (dotted curves). In the experiment, the distribution function is obtained from the differential conductance  $dI/dV(V)$  of the tunnel junction formed by the wire and a superconducting electrode placed underneath.

If, on the contrary, many inelastic collisions occur during the diffusion time, quasiparticles reach local thermal equilibrium. In this hot-electron regime, the distribution function is a Fermi function with electrochemical potential  $\mu(x) = -eUx$  and effective temperature  $T_{\text{eff}}(x) = \sqrt{T^2 + x(1-x)U^2/\mathcal{L}}$ , where  $\mathcal{L} = \frac{\pi^2}{3}(\frac{k_B}{e})^2$  is the Lorenz number [6,9] (see dotted lines in Fig. 1). In intermediate situations, the shape of the distribution function depends on the collision integral  $I_{\text{coll}}(x, E, \{f\})$ , thereby giving information on how quasiparticles interact [10].

The distribution function  $f(E) \equiv f(x_J, E)$  at the position  $x_J$  of the tunnel junction is related to the differential conductance of the junction through

$$\frac{dI}{dV}(V) = \frac{1}{R_T} \int dE \frac{\partial n_S}{\partial E}(E - eV) \times \{f(E) + \Theta(E - eV) - 1\}, \quad (3)$$

where  $R_T$  is the tunnel resistance of the junction,  $n_S(E) = \text{Re}(E/\sqrt{E^2 - \Delta^2})$  is the normalized BCS density of states with  $\Delta$  the energy gap of the superconducting electrode, and  $\Theta(E)$  is the Heaviside function. Equation (3) is written in the limit  $k_B T \ll \Delta$ . Effects of the electromagnetic environment [11] and the modification of the density of states due to interactions [12] have been neglected. The distribution function  $f(E)$  is obtained from the deconvolution of the measured  $dI/dV(V)$  using Eq. (3) [13].

All samples were fabricated by depositions at several angles through a germanium mask patterned with  $e$ -beam lithography [14]. The wires, made of copper, are 110 nm wide and 45 nm thick. Wire 1 and wire 2 were deposited simultaneously, and have lengths 1.5 and 5  $\mu\text{m}$ , respectively. Wire 3, fabricated separately, is also 5  $\mu\text{m}$  long. The electrodes at the ends of the wires are 500-nm-thick copper pads with an area of about 1  $\text{mm}^2$ , thereby implementing adequate reservoirs. The film forming the wires forms the bottom layer of the pads, which were thickened in a subsequent evaporation [10]. The superconducting probes, made of aluminum, were positioned in the middle of each wire. An additional superconducting probe was positioned 1.1  $\mu\text{m}$  away from the right end of wire 3. The areas of the tunnel junctions are  $300 \times 110 \text{ nm}^2$  in wires 1 and 2, and less than  $50 \times 50 \text{ nm}^2$  in wire 3. The samples were mounted in a copper box thermally anchored to the mixing chamber of a dilution refrigerator. Electrical connections were made through filtered coaxial lines [15], and measurements were carried out at a temperature of 25 mK. From the low-temperature resistances of wire 1 and 2, 14.5 and 53  $\Omega$ , we estimate the diffusion constant in the wires  $D \sim 65 \text{ cm}^2/\text{s}$  ( $\pm 10 \text{ cm}^2/\text{s}$ , given the uncertainties on the geometry) and the diffusion times  $\tau_D \sim 0.35 \text{ ns}$  and  $\tau_D \sim 4 \text{ ns}$ . Wire 3 is more resistive,  $R = 76 \Omega$ , yielding  $D \sim 45 \text{ cm}^2/\text{s}$  and  $\tau_D \sim 6 \text{ ns}$ .

The distribution functions in the center of wire 1 for  $U = 0, 0.1, \text{ and } 0.2 \text{ mV}$  are shown in the top left panel

of Fig. 2. They are obtained from the deconvolution of  $dI/dV(V)$  curves such as the one shown in the inset, which is taken at  $U = 0.2 \text{ mV}$ . The parameters for the deconvolution of the  $dI/dV(V)$  curves were obtained from a fit of Eq. (3) to the measured  $dI/dV(V)$  at  $U = 0$ , with  $f(E)$  a Fermi function. From the fit we find the value of the gap of our aluminum  $\Delta = 0.20 \text{ meV}$ , close to the bulk value, the tunnel resistance  $R_T = 10 \text{ k}\Omega$ , and the temperature of the Fermi function  $T = 30 \text{ mK}$ . This latter value is in reasonable agreement with the measured temperature  $T = 25 \text{ mK}$ . For  $U \neq 0$ , the functions  $f(E)$  resemble the staircase shape expected from Eq. (2). For comparison, we have plotted as a dotted line in Fig. 2 the predicted noninteracting quasiparticle distribution for  $U = 0.2 \text{ mV}$ . Deviations from the prediction of Eq. (2) are much more apparent in the data from wire 2 ( $L = 5 \mu\text{m}$ ), shown in the top right panel of Fig. 2 for the same values of  $U$ . As could be expected from the diffusion time through this wire which is more than 10 times greater than through wire 1, the distribution functions are more rounded. An almost complete thermalization of the quasiparticles occurs in wire 3, as shown by the distribution functions plotted in the bottom left panel

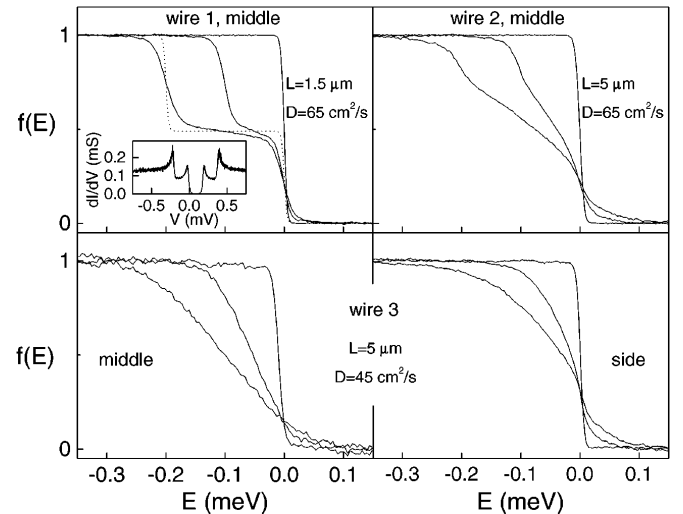


FIG. 2. Inset of the top left panel: Measured  $dI/dV(V)$  of the tunnel junction to wire 1 for  $U = 0.2 \text{ mV}$ . In the four panels, distribution functions, obtained from the deconvolution of such  $dI/dV(V)$  curves, for  $U = 0, 0.1, \text{ and } 0.2 \text{ mV}$  in the middle of a 1.5- $\mu\text{m}$ -long wire with a diffusion constant  $D \sim 65 \text{ cm}^2/\text{s}$  (wire 1, top left); in the middle of a 5- $\mu\text{m}$ -long wire with the same diffusion constant (wire 2, top right); in the middle (bottom left) and at 1.1  $\mu\text{m}$  from the grounded reservoir electrode (bottom right) of a 5- $\mu\text{m}$ -long wire (wire 3) with  $D \sim 45 \text{ cm}^2/\text{s}$ . Also plotted as a dotted line in the top left panel is the prediction for the noninteracting distribution function [Eq. (2)] for  $U = 0.2 \text{ mV}$ . All measurements were performed at 25 mK. The cross-sectional area of the three wires is nominally the same:  $45 \times 110 \text{ nm}^2$ . The tunnel resistances of the junctions were  $R_T = 10 \text{ k}\Omega$  for wires 1 and 2,  $R_T = 200 \text{ k}\Omega$  for the middle junction on wire 3, and  $R_T = 75 \text{ k}\Omega$  for the side junction on wire 3.

of Fig. 2. The curves of this latter panel can be fitted with a Fermi function at a temperature 5% higher than the effective temperature corresponding to the voltages  $U$  applied, given by  $T_{\text{eff}} = \sqrt{T^2 + U^2/4\Omega}$ . These distributions show that phonon emission, which would tend to cool the electrons below  $T_{\text{eff}}$ , can indeed be neglected. The fact that the observed temperatures are 5% higher than the calculated  $T_{\text{eff}}$  is consistent with an incomplete thermalization, as better seen from the distribution functions measured with the junction positioned 1.1  $\mu\text{m}$  away from the grounded reservoir, shown in the bottom right panel of Fig. 2. The kink in these curves at zero energy reflects the sharp discontinuity at zero energy of the Fermi distribution of the nearby reservoir, which has not been washed out by interactions at this distance.

A striking scaling property of the data is shown in Fig. 3 where the distribution functions, measured for voltages increasing from  $U = 0.05$  mV to  $U = 0.3$  mV by steps of 0.05 mV, are plotted as a function of the reduced parameter  $E/eU$ . Except for the smallest voltage  $U = 0.05$  mV, all the curves measured at a given position coincide. This property leads to a phenomenological expression for the collision integral in Eq. (1), as we now show.

The collision term  $I_{\text{coll}}(x, E, \{f\})$  in the Boltzmann equation is the difference of two terms: an in-collision term, the rate at which particles are scattered in the state of energy  $E$ , and an out-collision term:

$$I_{\text{coll}}(x, E, \{f\}) = I_{\text{coll}}^{\text{in}}(x, E, \{f\}) - I_{\text{coll}}^{\text{out}}(x, E, \{f\}) \quad (4)$$

with

$$I_{\text{coll}}^{\text{in,out}}(x, E, \{f\}) = \int d\varepsilon dE' dx' K(x, x', \varepsilon) f_{E+\varepsilon, E}^x \times (1 - f_{E, E-\varepsilon}^x) f_{E'}^{x'} (1 - f_{E'+\varepsilon}^{x'}), \quad (5)$$

where the shorthand  $f_E^x$  stands for  $f(x, E)$ . Following the Landau approach [1], we have assumed that the dominant process is a two-quasiparticle interaction. The kernel function  $K(x, x', \varepsilon)$  is proportional to the squared matrix element of the interaction during which an energy  $\varepsilon$  is transferred between two particles at positions  $x$  and  $x'$ . We assume that  $K(x, x', \varepsilon)$  depends only on  $\varepsilon$  since  $E \simeq E_F$ ,  $E' \simeq E_F$ , and  $\varepsilon \ll E_F$ . The energy dependence of  $K(x, x', \varepsilon)$  is inferred from the scaling property of the data, assuming that the scaling observed at the middle of all three wires and at the side position of wire 3 persists everywhere along each wire. Then, given that the steady-state distributions as well as the boundary conditions all depend on  $E/eU$  only (if  $k_B T \ll eU$ ), the collision integral must have the same property. Equation (5) then implies that  $U^2 K(x, x', \varepsilon)$  is a function of  $\varepsilon/eU$  only, yielding  $K(x, x', \varepsilon) = g(x, x')/\varepsilon^2$ , where  $g(x, x')$  is a function of space variables. When fitting the solution of Eq. (1), computed for  $eU \gg k_B T$ , to the experimental curves, we found that the shape of the simulated distribution functions is practically insensitive to the spatial extent of  $g(x, x')$ : taking a delta function or a constant produces the same shapes. In the following, we assume that the interaction is local, and  $g(x, x') \equiv \tau_0^{-1} \delta(x - x')$  where  $\tau_0^{-1}$  has the dimension of a rate. The shape of the distribution function is then determined by the ratio  $\tau_0/\tau_D$  only. The fits yield  $\tau_0/\tau_D = 2.5 \pm 0.2$  for wire 1,  $\tau_0/\tau_D = 0.3 \pm 0.05$  for wire 2, and  $\tau_0/\tau_D = 0.08 \pm 0.02$  for the lateral position on wire 3. The calculated distribution functions, plotted with open symbols in Fig. 3, account well for the measurements. We have taken for the middle position of wire 3 the same value  $\tau_0/\tau_D$  as for the side position, and find excellent agreement with the data. Given the additional uncertainties on the diffusion times, these results are compatible with an identical value  $\tau_0 \sim 1$  ns for wire 1 and wire 2, whereas we get  $\tau_0 \sim 0.5$  ns for wire 3. This is consistent with the assumption that the interaction is local, and that its strength does not depend on the length of the wire. The fact that the scaled  $U = 0.05$  mV curves do not coincide with the other scaled curves is explained by the rounding effect of the reservoir temperature, which is relatively more important at lower  $U$  [16].

In order to test the robustness of our determination of  $K(x, x', \varepsilon)$ , we have tried to fit our data with a different power law for  $K(x, x', \varepsilon)$ . We have found that exponents

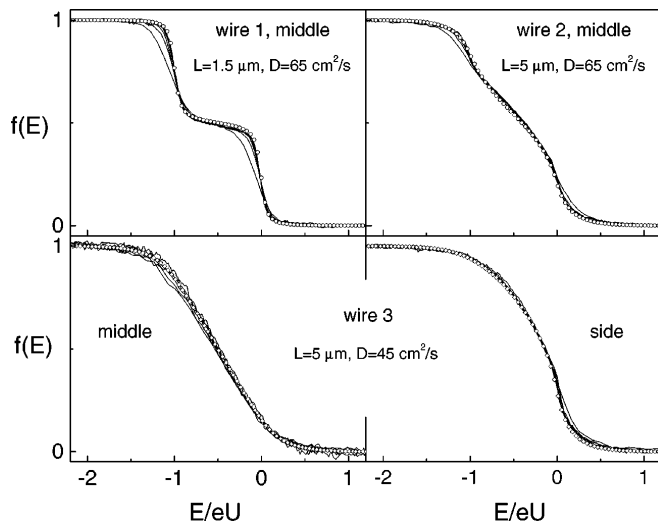


FIG. 3. Continuous lines in all four panels: distribution functions, for  $U$  ranging from 0.05 to 0.3 mV by steps of 0.05 mV, plotted as a function of the reduced energy  $E/eU$ , for the same positions as in Fig. 2. Open symbols are best fits of the data to the solution of the Boltzmann equation with an interaction kernel  $K(x, x', \varepsilon) = \tau_0^{-1} \delta(x - x')/\varepsilon^2$ : in top panel, open circles correspond to the calculated distribution function in the middle of wires 1 and 2 ( $x = 0.5$ ), with  $\tau_0/\tau_D = 2.5$  and  $\tau_0/\tau_D = 0.3$ , respectively (both compatible with  $\tau_0 \sim 1$  ns). In bottom panels, open diamonds are computed at  $x = 0.5$  and  $x = 0.25$  with  $\tau_0/\tau_D = 0.08$  ( $\tau_0 \sim 0.5$  ns).

of  $\varepsilon$  differing from  $-2$  by more than  $0.1$  are incompatible with the scaling displayed by the data. In addition, we have found that the distribution function is practically insensitive to the interaction law below  $eU/4$ . The data presented here therefore impose  $K(x, x', \varepsilon) \propto 1/\varepsilon^{2 \pm 0.1}$  in the energy range  $(E_0, 0.30 \text{ meV})$  with  $E_0 \leq 0.01 \text{ meV}$ .

This energy dependence differs from the prediction  $K(x, x', \varepsilon) \propto \varepsilon^{-3/2}$  of the direct calculation of the screened Coulomb interaction between quasiparticles in a homogeneous diffusive medium in the 1D regime [3]. However, the  $1/\varepsilon^2$  dependence can be obtained from another calculation in which the quasiparticle interactions are treated by considering the coupling between a quasiparticle and the fluctuating electromagnetic field produced by all the others. This point of view was already successfully used to calculate the dephasing time of a given quasiparticle when the others are in thermal equilibrium [3,17]. In a generalization of this reasoning, we treat the energy transfer between quasiparticles with an arbitrary distribution function, and consider the fluctuations of the electromagnetic field at the scale of the elastic mean free path [18].

Finally, let us mention that our result  $K(x, x', \varepsilon) = \tau_0^{-1} \delta(x - x')/\varepsilon^2$  in the experimental energy window  $(E_0, 0.30 \text{ meV})$  implies an upper bound for the quasiparticle lifetime. For  $E$  within this energy range, we obtain  $\tau(E) < \tau_0/\ln(E/E_0)$ , where  $\tau_0 \sim 1 \text{ ns}$ . At  $E = 0.1 \text{ meV}$ , this upper bound is 2 orders of magnitude shorter than the quasiparticle lifetime predicted in diffusive 1D metals [3] with the same diffusion constants as in our samples. Further experiments are needed to clarify this issue.

We acknowledge L. Calvet and F. Pierre for their contributions to the experiment, and Ya. Blanter for valuable discussions. This work was partially supported by the Bureau National de la Métrologie. N.O.B. acknowledges support of the NSF under Grant No. DMR-9321850.

---

\*Permanent address: Michigan State University, East Lansing, MI 48824.

- [1] D. Pines and P. Nozière, *The Theory of Quantum Liquids* (W.A. Benjamin, New York, 1966).
- [2] *Mesoscopic Quantum Physics*, edited by E. Akkermans, G. Montambaux, J.-L. Pichard, and J. Zinn-Justin, (North-Holland, Amsterdam, 1991).
- [3] For a review, see B.L. Altshuler and A.G. Aronov, in *Electron-Electron Interactions in Disordered Systems*,

- edited by A.L. Efros and M. Pollak (Elsevier Science Publishers B.V., City, 1985).
- [4] W.S. Fann, R. Storz, H.W.K. Tom, and J. Bokor, *Phys. Rev. B* **46**, 13 592 (1992).
- [5] C.G. Smith and M.N. Wybourne, *Solid State Commun.* **57**, 411 (1986); F.C. Wellstood, C. Urbina, and John Clarke, *Phys. Rev. B* **49**, 5942 (1994).
- [6] A.H. Steinbach, J.M. Martinis, and M.H. Devoret, *Phys. Rev. Lett.* **76**, 3806 (1996); R.J. Schoelkopf, P.J. Burke, A. A. Kozhevnikov, D.E. Prober, and M.J. Rooks, *Phys. Rev. Lett.* **78**, 3370 (1997).
- [7] R. Landauer, *IBM J. Res. Dev.* **1**, 223 (1957); **32**, 306 (1988).
- [8] K.E. Nagaev, *Phys. Lett. A* **169**, 103 (1992); *Phys. Rev. B* **52**, 4740 (1995).
- [9] V.I. Kozub and A.M. Rudin, *Phys. Rev. B* **52**, 7853 (1995).
- [10] A detailed discussion of the different regimes, as well as details of the sample fabrication and preliminary experimental results, can be found in H. Pothier, S. Guéron, Norman O. Birge, D. Esteve, and M.H. Devoret, *Z. Phys. B* **104**, 178 (1997).
- [11] G.-L. Ingold and Yu.V. Nazarov, in *Single Charge Tunneling*, edited by H. Grabert and M.H. Devoret (Plenum Press, New York, 1992), p. 21.
- [12] The relative corrections to the density of states predicted in Ref. [3] are at most of the order of 1% in our copper wires. Experimentally, our neglecting this effect is justified by the good fit of our data at  $U = 0$  with Eq. (3) in which  $f(E)$  is a Fermi function.
- [13] In the experiment,  $R_T$  is more than 200 times the resistance of the wire, and we measure  $\frac{dI}{dV}(V)$  with  $V$  of the order of  $U$ , so that the perturbation induced by the probe current can be neglected.
- [14] By a selective etching of the polymer underneath the mask, we could control which features of the pattern were reproduced on the substrate for each evaporation. This was achieved by a low-dose electronic exposure of the regions where the polymer below the stencil needed to be dissolved.
- [15] D. Vion, P.F. Orfila, P. Joyez, D. Esteve, and M. H. Devoret, *J. Appl. Phys.* **77**, 2519 (1995).
- [16] The experimental curves are well fitted (data not shown) by taking  $T_{\text{res}} = 50 \text{ mK}$  for wire 1 and  $T_{\text{res}} = 35 \text{ mK}$  for wires 2 and 3. The reservoir temperature  $T_{\text{res}}$  is higher than the phonon temperature due to the injected power from the wires (see Ref. [5]).
- [17] B.L. Altshuler, A.G. Aronov, and D.E. Khmel'nitskii, *J. Phys. C* **15**, 7367 (1982).
- [18] M.H. Devoret, D. Esteve, S. Guéron, and H. Pothier (to be published).